ISSN 1069-3513, Izvestiya, Physics of the Solid Earth, 2006, Vol. 42, No. 9, pp. 734–744. © Pleiades Publishing, Inc., 2006.
Original Russian Text © A.A. Lyubushin, G.A. Sobolev, 2006, published in Fizika Zemli, 2006, No. 9, pp. 18–28.

Multifractal Measures of Synchronization of Microseismic Oscillations in a Minute Range of Periods

A. A. Lyubushin and G. A. Sobolev

Schmidt Institute of Physics of the Earth, Russian Academy of Sciences (RAS), Bol'shaya Gruzinskaya ul. 10, Moscow, 123995 Russia

Received January 30, 2006

Abstract—The paper considers synchronous continuous records of microseismic background obtained within a month before the Kronotskii (Kamchatka) December 5, 1997, earthquake ($M = 7.8$) at six IRIS broadband stations that are located in a large region extending from central European Russia (the town of Obninsk) to the Far East (Kamchatka and Sakhalin). By averaging and downsampling, initial records were discretized at an interval of 30 s and the microseismic background was examined in the range of periods from 1 min to 2.4 h, after scale-dependent trends due to the effects of tides and temperature variations had been removed. Microseismic fluctuations were analyzed with the help of estimates of the evolution of their multifractal singularity spectra in a moving time window 12 h wide. As the criterion characterizing the background properties in a current time window, we took the values of the generalized Hurst exponent α^* realizing the maximum of the singularity spectrum. Hidden synchronization effects of a microseismic field preceding a seismic event are identified by estimating the evolution of the spectral measure of coherent behavior of α^* variations in a moving time window 5 days long for various combinations of jointly analyzed stations.

PACS numbers: 91.30.Px

DOI: 10.1134/S1069351306090035

INTRODUCTION

The analysis of fractal and multifractal properties of geophysical monitoring time series is a promising direction of data analysis in the physics of the solid Earth [Smirnov et al., 2005; Currenti et al., 2005; Ramírez-Rojas et al., 2004; Telesca et al., 2005; Turcotte, 1997]. This is due to the fact that the fractal analysis can effectively explore signals that, in terms of covariance and spectral theory, are no more than white noise or Brownian motion. One of the first papers using the analysis of fractal properties of time series was the work by H.E. Hurst on the year-average river runoff [Hurst, 1951; Feder, 1988; Mandelbrot and Wallis, 1969]. The empirical law of Hurst is the validity of the relation $R(\tau)/\sigma(\tau) \sim \tau^H$, where $R(\tau)$ is the difference between the maximum and the minimum increments in the observed value in the τ-long time interval, $\sigma(\tau)$ is the standard deviation, and $0 < H < 1$ is a constant whose value is close to 0.7 for the majority of meteorological and hydrological observations. In the case of a self-similar process $X(t)$, the average of squared increments meets the condition $\langle|X(t + \delta t) - X(t)^2\rangle \sim |\delta t|^{2H}$ and the frequency dependence of the power spectrum obeys a power law: $S_{XX}(\omega) \sim \omega^{-(2H+1)}$, $\omega \longrightarrow 0$.

A further generalization of this model is the dependence of the Hurst constant on time, i.e., the consideration of a random process such that $\langle|X(t + \delta t) - X(t)^2\rangle \sim |\delta t|^{2H}$, $0 < H(t) < 1$. This generalization was proposed by Mandelbrot [Mandelbrot, 1983; Feder, 1988] and was called multifractal Brownian motion described by the distribution of probabilities of $H(t)$ values, or the so-called multifractal singularity spectrum. The singularity spectrum is an informative statistic characterizing the regime of chaotic fluctuations in the observed value.

This work continues a series of papers devoted to the analysis of microseisms using various approaches. Sobolev [2004] analyzed the periodic structure of microseismic pulsations in a moving time window by the method proposed in [Lyubushin et al., 1998] for the identification of periodic components in a point process. These studies were continued in [Sobolev et al., 2005], where the structure of low frequency (a minute range of periods) variations in the microseismic background was additionally analyzed using orthogonal wavelet expansions. Below, the low frequency seismic background is examined through the transition to the analysis of variations in the singularity spectra of noise fluctuations and moving time window estimates of the coherence measures of variations in spectral singularity characteristics for observations at different stations. The final goal is the recovery of hidden synchronization effects in the field of microseismic vibrations in large regions prior to strong earthquakes.

DATA OF MICROSEISMIC OSCILLATIONS

We considered 20-Hz discretized data on the vertical component recorded at six IRIS broadband stations in Petropavlovsk-Kamchatski (Pet), Yuzhno-Sakhalinsk (Yss), Magadan (Mag), Yakutsk (Yak), Arti in the Urals (Aru), and Obninsk (Obn) during one month from November 5 to December 5, 1997, strictly before the Kronotskii (Kamchatka) earthquake (M = 7.8) of December 5, 1997; the seismic records were kindly afforded by the RAS Geophysical Service. The three-letter codes of the stations are used everywhere below. For the transition to a minute range of periods, the initial records were averaged and downsampled by 600 times, which gave time series with a discretization interval of 30 s. These records contained high amplitude pulsations caused by arrivals from either far strong earthquakes or local events, including industrial blasts. To eliminate spurious effects due to such pulsations, the 30-s discretized data were processed by the iterative winzorization procedure used in robust statistics [Huber, 1981]; the procedure consists in the calculation of the average $\bar{x}$ and standard deviation σ and the clipping of time series values lying beyond the interval $\bar{x} \pm 4\sigma$, and this succession of three operations is repeated until the values $\bar{x}$ and σ stop varying.

Figure 1 plots the data obtained after the averaging, thinning, and winzorization. The plots clearly show tidal vibrations and other low frequency trends, supposedly related to variations in temperature and atmospheric pressure. Note that the Yak record contains a data gap in the interval 20 160–21 598 min, observed in Fig. 1 as a plateau of constant values. Moreover, the Aru record contains a low frequency anomaly (possibly, a calibrating pulse) encompassing the interval 32 200–32 960 min and followed by significant upward and downward jumps with the subsequent gradual recovery of the average level. These two data defects should be kept in mind when interpreting results of the analysis. Note that Aru data interval with a strongly increasing trend following a low frequency pulse is quite suitable for analysis because the method used for estimating the singularity spectrum is designed to eliminate the influence of trends. The plateaus of constant values were perturbed by weak Gaussian white noise with a variance of 10^{-3} in order that the method used for estimating the singularity spectrum in a moving time window could be applied continuously throughout the Yak and Aru records without stopping in the defective intervals of constant values due to numerical instability.

ESTIMATION OF THE SINGULARITY SPECTRUM

Presently, two approaches are used for estimating singularity spectra of a time series. The first, earlier method is based on the analysis of point chains of the maximum moduli of continuous wavelet transformations with wavelets usually equal to the derivatives of various orders of the Gaussian distribution density function [Bacry et al., 1993; Mallat, 1998; Muzy, 1994]. The second approach is closer to the Hurst technique and is based on the analysis of the dependence of the standard deviation or sample peak-to-valley value on the sample length. A method of analysis of fluctuations after elimination of scale-dependent trends, or the detrended fluctuation analysis (DFA), has recently been developed and widely applied in various applications [Kantelhardt et al., 2002, 2003]. The comparative analysis of the application of these methods shows that the DFA method is more reliable and stable. However, the DFA method is unsuitable for self-similar signals of a special form that can contain plateaus of constant values (of the type of the well-known devil's staircase constructed on the basis of the Cantor set), and the estimation using continuous wavelet transformations is preferable. In this paper, we used the DFA method, which is most suitable for the analysis of highly variative microseismic noise. Below, we briefly describe the essence of the method.

Let $X(t)$ be a random process. As the measure of the behavior of the signal $X(t)$ in the interval $[t, t + \delta]$, we define the signal increment modulus $\mu_X(t, \delta) = |X(t + \delta) - X(t)|$ and calculate the average modulus of such measures raised to power q:

$$M(\delta, q) = M\{(\mu_X(t, \delta))^q\}. \quad (1)$$

A random process is scale invariant if $M(\delta, q) \sim |\delta|^{\kappa(q)}$ as $\delta \longrightarrow 0$, i.e., if there exists the limit

$$\kappa(q) = \lim_{\delta \to 0} \frac{\ln M(\delta, q)}{\ln|\delta|}. \quad (2)$$

Note that, in definition (1)–(2), the peak-to-valley value can be taken as the measure $\mu_X(t, \delta)$, which is closer to Hurst's traditional constructions:

$$\mu_X(t, \delta) = \max_{t \le s \le t+\delta} X(s) - \min_{t \le s \le t+\delta} X(s). \quad (3)$$

If the dependence $\kappa(q)$ is linear, $\kappa(q) = Hq$, where H = const, $0 < H < 1$, then the process is monofractal. In particular, we have $H = 0.5$ for the classical Brownian motion.

The DFA method can be applied to the calculation of $\kappa(q)$ using a finite sample from the time series $X(t)$, $t = 1, \ldots, N$ [Kantelhardt et al., 2002]. Let s be the number of samples that is associated with the varied scale δ_s: $\delta_s = s\Delta t$. We divide the sample into nonoverlapping small intervals s samples in length,

$$I_k^{(s)} = \{t: 1 + (k-1)s \le t \le ks, \ k = 1, \ldots, [N/s]\}, \quad (4)$$

and let

$$y_k^{(s)}(t) = X((k-1)s + t), \quad t = 1, \ldots, s, \quad (5)$$

be the segment of the time series $X(t)$ corresponding to the interval $I_k^{(s)}$. Let $p_k^{(s, m)}(t)$ be a polynomial of order m fitted by the least squares method to the signal $y_k^{(s)}(t)$. We consider deviations from the local trend

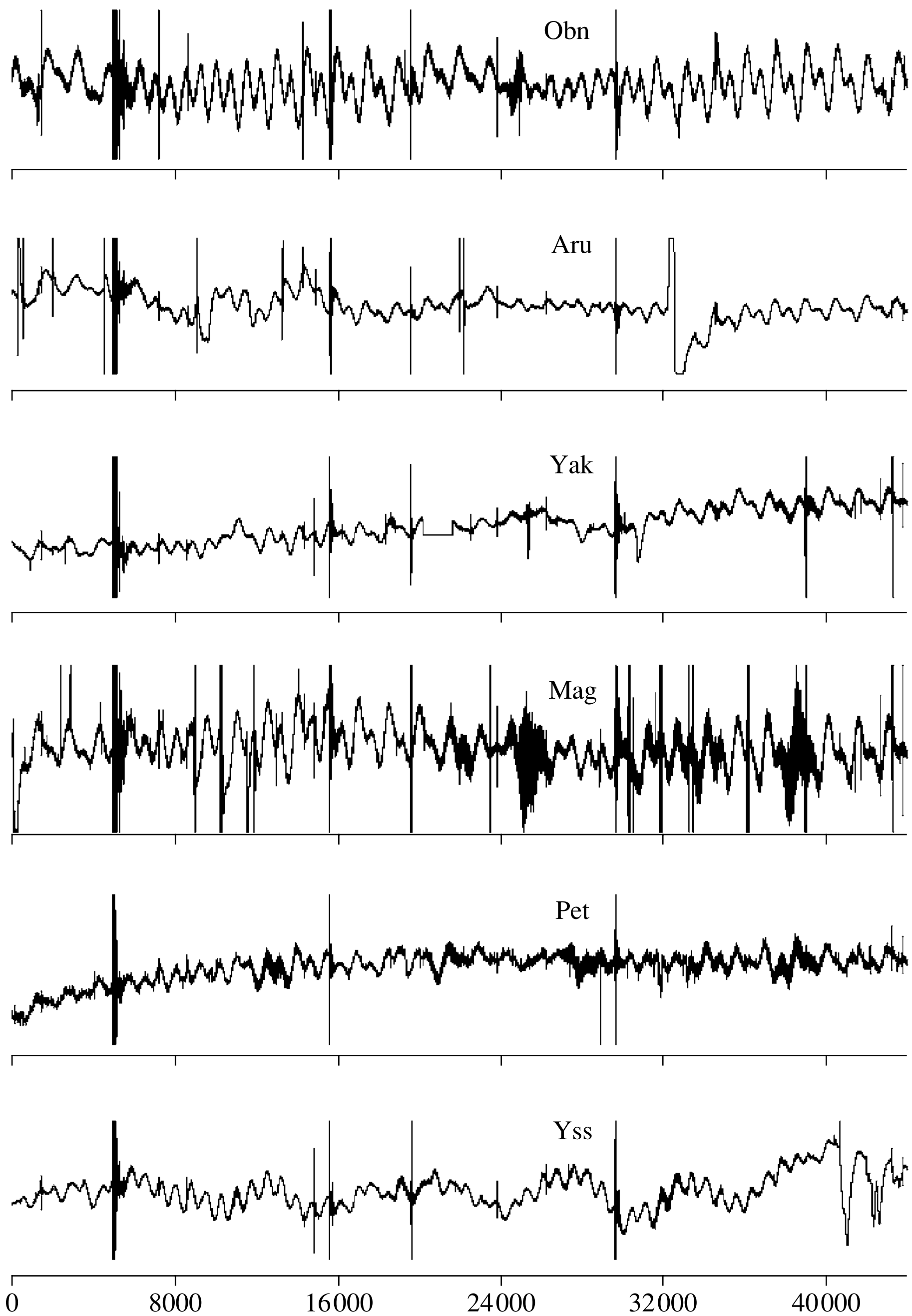

Fig. 1. Plots of initial data from six stations (their codes are shown in the figure) after both their 30-s discretization and the application of the winzorization operation (iterative truncation of large pulsations in data due to arrivals from earthquakes).

$$\Delta y_k^{(s,m)}(t) = y_k^{(s)}(t) - p_k^{(s,m)}(t), \quad t = 1, \dots, s, \quad (6)$$

and calculate the value

$$Z^{(m)}(q,s) = \left(\sum_{k=1}^{[N/s]} (\max_{1 \le t \le s} \Delta y_k^{(s,m)}(t) - \min_{1 \le t \le s} \Delta y_k^{(s,m)}(t))^q / [N/s] \right)^{1/q}, \quad (7)$$

which will be regarded as an estimate for $M(\delta_s, q)^{1/q}$. The procedure of trend elimination in each small segment s samples in length is necessary if trends of external origin (seasonal, tidal, and so on) are present in the signal. Now, we define the function $h(q)$ as the coefficient of linear regression between the values $\ln(Z^{(m)}(q, s))$ and $\ln(s)$: $Z^{(m)}(q, s) \sim s^{h(q)}$. It is evident that $\kappa(q) = qh(q)$, whereas $h(q) = H = \text{const}$ for a monofractal process.

The next step in the multifractal analysis [Feder, 1988] after the determination of the function $\kappa(q)$ is the calculation of the singularity spectrum $F(\alpha)$, which is the average fractal dimension of the set of points in the vicinity of which the Goelder–Lipshitz exponent of random realizations of the process $X(t)$ is α, i.e., the set of the points t such that $|X(t+\delta) - X(t)| \sim |\delta|^{\alpha}$, $\delta \longrightarrow 0$. The standard approach consists in the calculation of the Gibbs statistical sum

$$W(q, s) = \sum_{k=1}^{[N/s]} (\max_{1 \le t \le s} \Delta y_k^{(s, m)} - \min_{1 \le t \le s} \Delta y_k^{(s, m)}(t))^q \quad (8)$$

and the determination of the mass indicator $\tau(q)$ from the condition $W(q, s) \sim s^{\tau(q)}$, after which the spectrum $F(\alpha)$ is calculated by the formula

$$F(\alpha) = \max\{\min_q(\alpha q - \tau(q)), 0\}. \quad (9)$$

Comparing (6) and (8), it is readily seen that $\tau(q) = \kappa(q) - 1 = qh(q) - 1$.

Thus, we have $F(\alpha) = \max\{\min_q(q(\alpha - h(q)) + 1, 0\}$. In the case of a multifractal process, when $h(q) = H +$ const, we obtain $F(H) = 1$ and $F(\alpha) = 0\ \forall \alpha \ne H$.

If the spectrum $F(\alpha)$ is estimated in a moving window, its evolution can give information on the variation in the structure of chaotic pulsations of the series. In particular, the position and width of the support of the spectrum $F(\alpha)$, i.e., the values $\alpha_{\min}$, $\alpha_{\max}$, $\Delta\alpha = \alpha_{\max} - \alpha_{\min}$, and α^* ($F(\alpha^*) = \max_\alpha F(\alpha)$) are characteristics of the noise. The value α^* can be called a generalized Hurst exponent. In the case of a monofractal signal, the quantity $\Delta\alpha$ should vanish and $\alpha^* = H$. As regards the value of $F(\alpha^*)$, it is equal to the fractal dimension of points in the vicinity of which the scaling relation $M(\delta, q) \sim |\delta|^{\kappa(q)}$ holds true. Usually $F(\alpha^*) = 1$, but there exist windows for which $F(\alpha^*) < 1$. We remind the reader that, in the general case (not only in the analysis of time series), $F(\alpha^*)$ is equal to the fractal dimension of the multifractal measure support [Feder, 1988].

MEASURE OF SYNCHRONIZATION OF VARIATIONS IN SINGULARITY SPECTRA

The analysis aims to recover effects of the coherent (synchronous) behavior of microseismic noise in a minute range of periods after the initial data are transformed into their singularity spectra estimated in a moving time window. The quantity chosen below as the characteristic of a singularity spectrum is the value α^* of the argument at which the spectrum attains its maximum. The values α^* characterize the most typical singularity that recurs most frequently within the current window, provided that the behavior of the noise component of microseisms is self-similar.

To obtain time series describing the evolution of the α^* values, we chose a moving window of a width of 1440 30-s samples (i.e., 12 h) with a shift 120 samples (1 h) long. Fourth-degree polynomials were taken to eliminate scale dependent trends with the use of formula (6). The function $h(q)$ in the relation $Z^{(m)}(q, s) \sim s^{h(q)}$ was estimated in each window for scales s varying from a minimum value of 20 samples to a maximum equal to one-fifth of the window width. Therefore, given a width of 1440 samples, the maximum scale is equal to 288 30-s samples, or 144 min (2.4 h).

Figure 2 plots the data after the elimination of local fourth-degree polynomial trends in a moving window of a radius of 144 samples, which is approximately equal to the maximum scale considered in estimating the function $h(q)$; these plots give an idea of which noise component of microseisms is actually examined after the trend elimination. Figure 3a presents the plots of the singularity spectra obtained with the first time window from Obninsk data. Figure 3b presents plots of both the values $\log(Z^{(m)}(q, s))$ and linear trends approximating them for ten various values of the exponent q with the same time window. The slope of the linear trends is nothing else than the function $h(q)$, whose values are used for calculating the mass indicator $\tau(q) = qh(q) - 1$ and then, according to formula (9), the singularity spectrum itself. Figure 3b demonstrates that the dependence of $\log(Z^{(m)}(q, s))$ versus $\log(s)$ is well consistent with a linear law, implying that seismic noise is self-similar. If the signal were monofractal, the trend lines would be parallel to each other. Figure 4 illustrates the evolution of the α^* values for each of the six stations as a function of the right-hand end of the moving time window.

The further analysis aims at the discovery of coherent variations in the α^* values. The strong correlation between the Yak and Mag variations in α^* beginning from the time 38000 min is observed even visually. To extract more hidden coherences that can be shifted in phase and involve a few stations, we applied the method using the estimation of canonical coherences in a moving time window developed in [Lyubushin, 1998] for the detection of earthquake precursors from geophysical monitoring data. This method was applied in [Lyubushin et al., 2003, 2004] to the analysis of multivariate hydrological and oceanographic (water-level valued) time series. The method consists in the estimation of the frequency dependent measure of the coherent behavior of components of multivariate time series, and its essentials are outlined below.

The ordinary spectrum of coherence of two processes can be unrigorously defined as the squared coefficient of correlation of these processes at a frequency ω [Jenkins and Watts, 1968]. The canonical coherence extends the notion of the coherence spectrum to the situation where one should explore not a pair of scalar time series but the relation at various frequencies

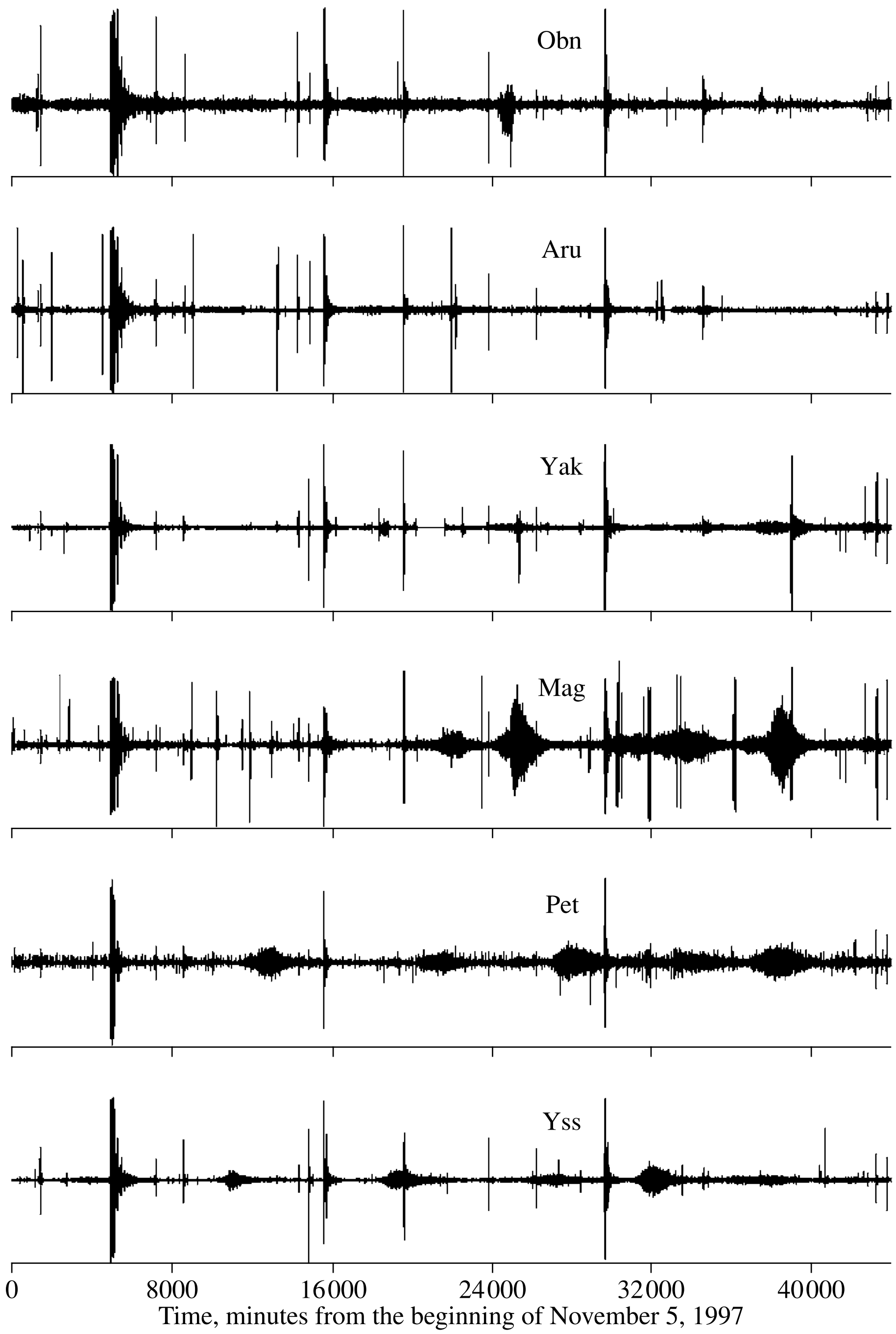

Fig. 2. Plots of the analyzed microseismic background at all stations after the removal of local fourth-degree polynomial trends in the moving time window of a radius of 144 samples.

between two vector time series, the *m*-dimensional series $X(t)$ and the *n*-dimensional series $Y(t)$. The value $\mu_1^2(\omega)$, called the squared modulus of the first canonical coherence of the series $X(t)$ and $Y(t)$, in this case plays the role of the ordinary spectrum of coherence and is calculated as the maximum eigenvalue of the matrix [Brillinger, 1975; Hannan, 1970]

$$U(\omega) = S_{xx}^{-1}(\omega)S_{xy}(\omega)S_{yy}^{-1}(\omega)S_{yx}(\omega). \qquad (10)$$

Here, t is the discrete time enumerating the successive samples; ω is frequency; $S_{xx}(\omega)$ is the spectral $m \times m$ matrix of the power series $X(t)$; and $S_{xy}(\omega)$ is the cross-spectral rectangular $m \times n$ matrix, $S_{yx}(\omega) = S_{xy}^H(\omega)$ (the subscript "H" means Hermitean conjugation).

We introduce the notion of component canonical coherences $\nu_i^2(\omega)$ of a q-dimensional time series $Z(t)$

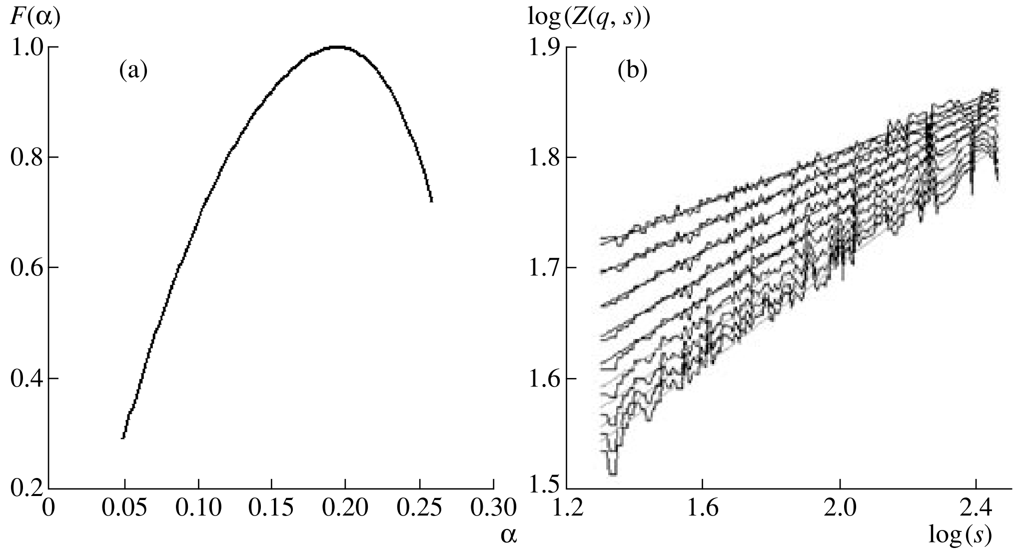

Fig. 3. Plots of the multifractal singularity spectrum $F(\alpha)$ (a) and the dependences of the statistical sum $\log(Z^{(m)}(q, s))$ versus $\log(s)$ (b) obtained with the first time window 12 h wide from Obninsk record data. The dependences in Fig. 3b are approximated by linear trends with the following values of the degree q (from top to bottom): 10, 7.5, 5, 2.5, –0.05, –2.5, –5, –7.5, and –10.

($q \geq 3$) defined as the squared moduli of the first canonical coherence in the case when $Y(t)$ in formula (9) is the ith scalar component of the q-dimensional series $Z(t)$, and $X(t)$ is the $(q-1)$-dimensional series consisting of the other components. Therefore, the value $\nu_i^2(\omega)$ characterizes the coherence, at the frequency ω, of variations of the ith component with variations of all other components. The introduction of component canonical coherences allows one to define one more frequency dependent statistic $\lambda(\omega)$ characterizing the coherence between variations of all components of the vector series $Z(t)$ at the frequency ω:

$$\lambda(\omega) = \prod_{i=1}^{q} \nu_i(\omega). \tag{11}$$

Note that, by definition, the quantity $\lambda(\omega)$ lies in the interval [0, 1], and the closer its value to unity, the stronger the coherence between variations of the components of the multivariate series $Z(t)$ at the frequency ω. We should emphasize that the comparison of absolute values of the statistic $\lambda(\omega)$ is possible only for the same number q of simultaneously processed time series because, by virtue of formula (11), with increasing q, the value λ decreases as the product of q values smaller than unity. If $q = 2$, measure (11) is the ordinary squared modulus of the coherence spectrum.

In order to estimate the temporal variability of the coherence between the recorded processes, calculations should be made in a moving time window of a given width. Let τ be the time coordinate in the window L samples wide. Calculating spectral matrices for samples in the time window τ, we obtain the two-parametric function $\lambda(\tau, \omega)$. Peaks in the value $\lambda(\tau, \omega)$ define the frequency bands and time intervals of an increase in the collective behavior of the jointly analyzed processes.

To implement this algorithm, an estimate of the spectral $q \times q$ matrix $S_{zz}(\tau, \omega)$ should be available in each time window. Below, we prefer the use of the vector autoregression model [Marple, 1987]. The method consists in the estimation of the model parameters:

$$Z(t) + \sum_{k=1}^{p} A_k Z(t-k) = e(t). \tag{12}$$

Here, A_k is the $q \times q$ matrix of autoregression parameters; p is the autoregression order; and $e(t)$ is the q-dimensional time series of identification residuals, which is assumed to be a sequence of independent Gaussian vectors with a zero mean and an unknown covariance matrix P. It is noteworthy that model (12) was constructed after the preliminary operations of the removal of the general linear trend, the transition to increments (to enhance the stationarity in narrow time windows), and the normalization of each scalar component to the unit variance. These operations were performed independently in each processing time window and for each scalar component of the multidimensional series. Their aim is to eliminate the influence of the difference in scales of the series processed. To estimate the matrices A_k and P, we used the recurrent Darbin–Levinson procedure [Marple, 1987], which requires the preliminary calculation of sample estimates of the covariance matrices.

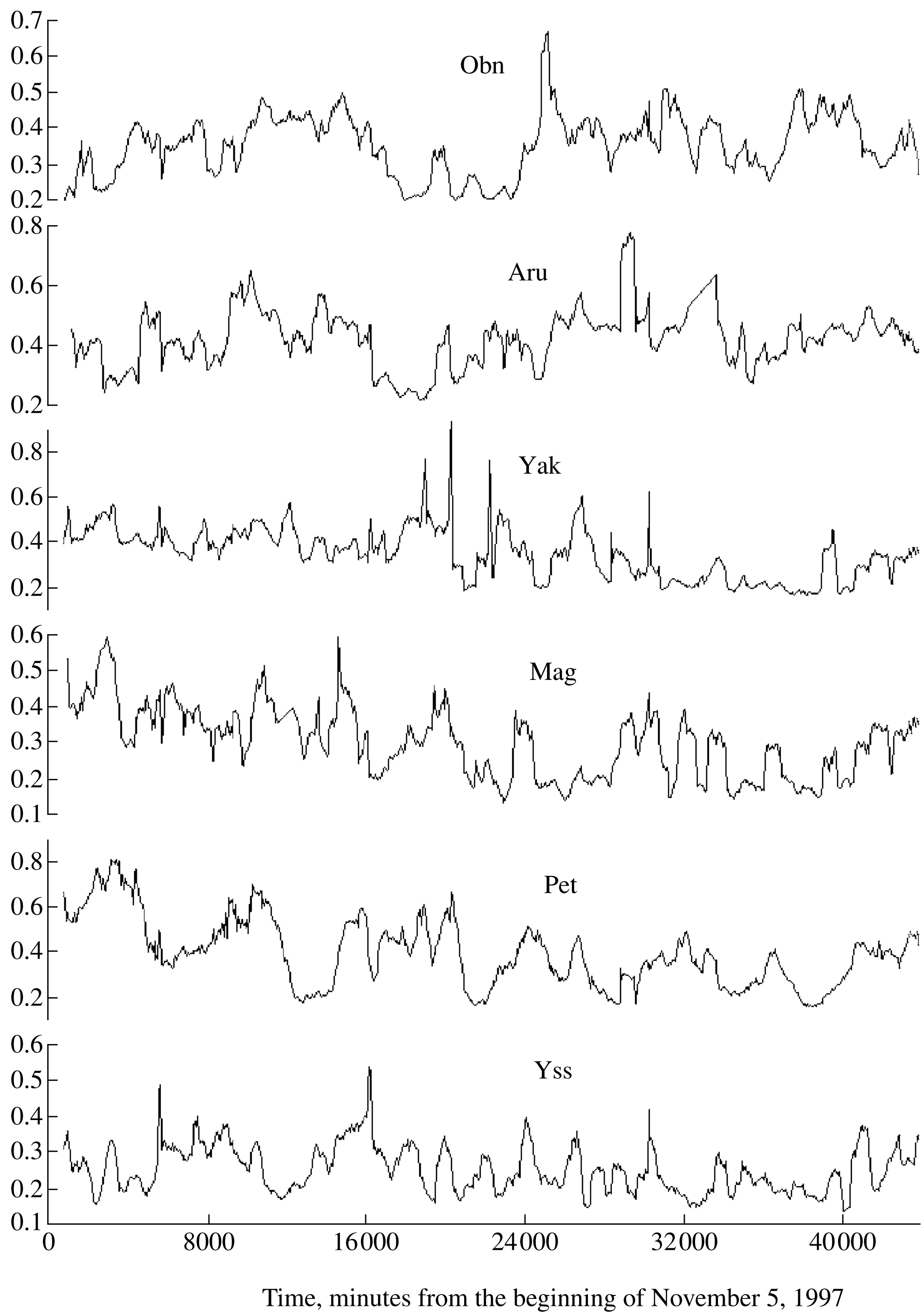

Fig. 4. Plots of the generalized Hurst exponent α^* realizing the maximum of the singularity spectrum of the microseismic background at all stations with the estimation in a moving time window 12 h wide with a shift of 1 h. The coordinate of the right-hand end of the moving time window is plotted on the time axis.

The estimate of the spectral matrix is calculated by the formula

$$S_{zz}(\omega) = F^{-1}(\omega)PF^{-H}(\omega),$$
$$\text{where } F(\omega) = I + \sum_{k=1}^{p} A_k \exp(-i\omega k). \quad (13)$$

Estimate (13) has a good resolution in frequency for short samples and is, therefore, preferable for estimations in a moving window as compared, for example, with nonparametric estimations through the averaging of multidimensional periodograms. No reliable formalized procedures exist for the choice of the autoregression order p. In our calculations, p was chosen by the

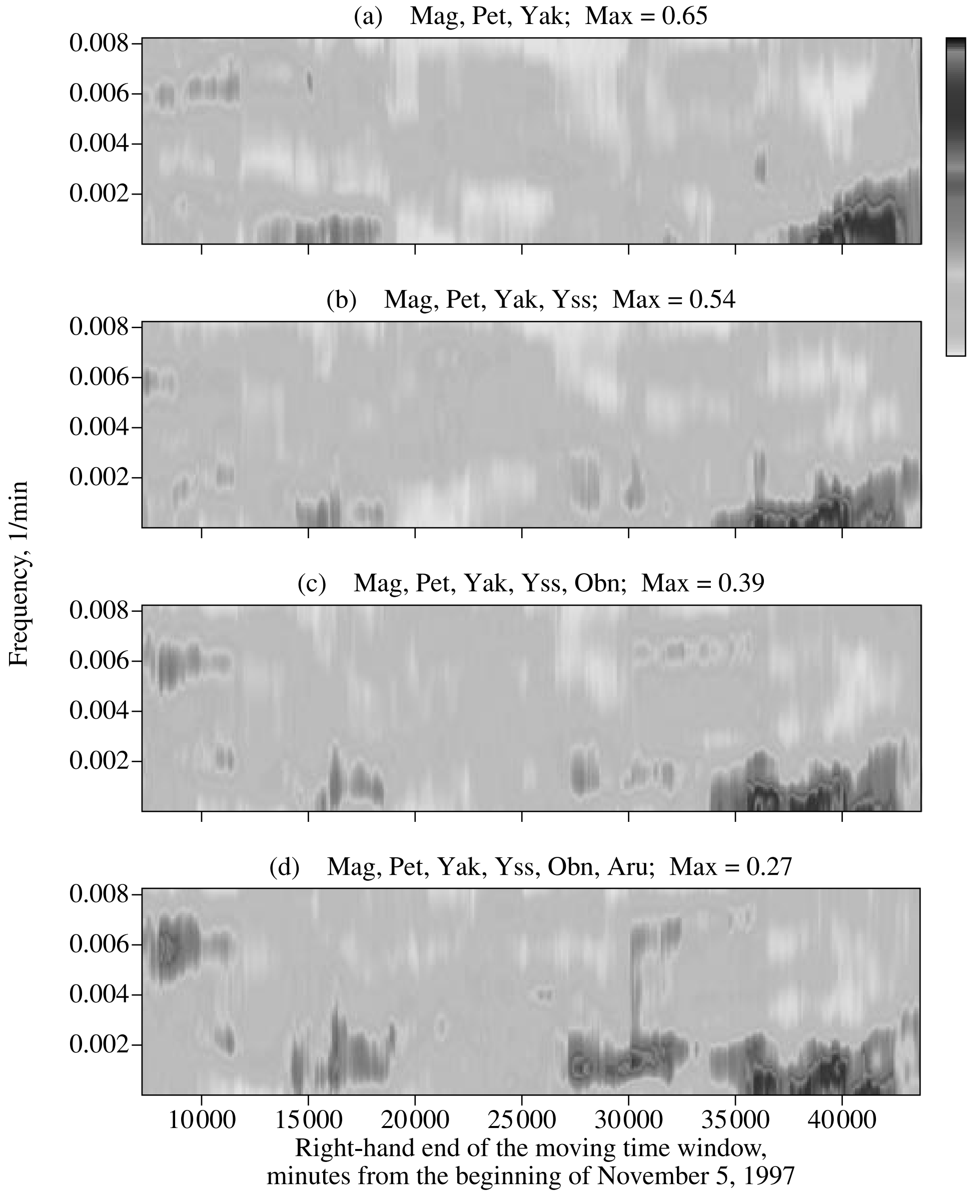

Fig. 5. Frequency–time diagrams of the evolution of the spectral measure of coherence of α* variation spectral series with the estimation in the moving time window 109 samples (5 days) long for a successively increasing number of simultaneously analyzed stations. Maximum values of the coherence measure are shown in each diagram after the codes of the stations analyzed.

trial-and-error method as a minimum value such that its further increase does not change significantly the main behavior patterns of the dependence $\lambda(\tau, \omega)$. Everywhere below we use the value $p = 3$.

The width of the time window used for the calculation of the dependence $\lambda(\tau, \omega)$ was set equal to 109 discrete values. Since each value of α* was obtained with the time window 12 h wide with a shift of 1 h, the width of the time window used for estimating the spectral matrix is $(109 - 1) \times 1 + 12 = 120$ h = 5 days. Figures 5 and 6 plot 2-D dependences $\lambda(\tau, \omega)$ obtained for combinations of the time series of α* variations recorded at various stations.

INTERPRETATION OF FREQUENCY–TIME COHERENCE DIAGRAMS

First of all, note that the intense synchronous noise pulsation in the interval 4920–6000 min (Fig. 2) due to the arrival from the far strong ($M = 7.9$) earthquake of November 8, 1997, 10:02 GMT (35.08°N, 87.32°E), gave an increase in the coherence measure of α* variations observed only in Figs. 5d and 6a and only at "high" frequencies with a period of about 160 min. Figure 2 exhibits a few other similar synchronous pulsations that also gave an insignificant increase in the measure $\lambda(\tau, \omega)$. Very insignificant synchronous variations in Fig. 2, including two foreshocks, are observed at the

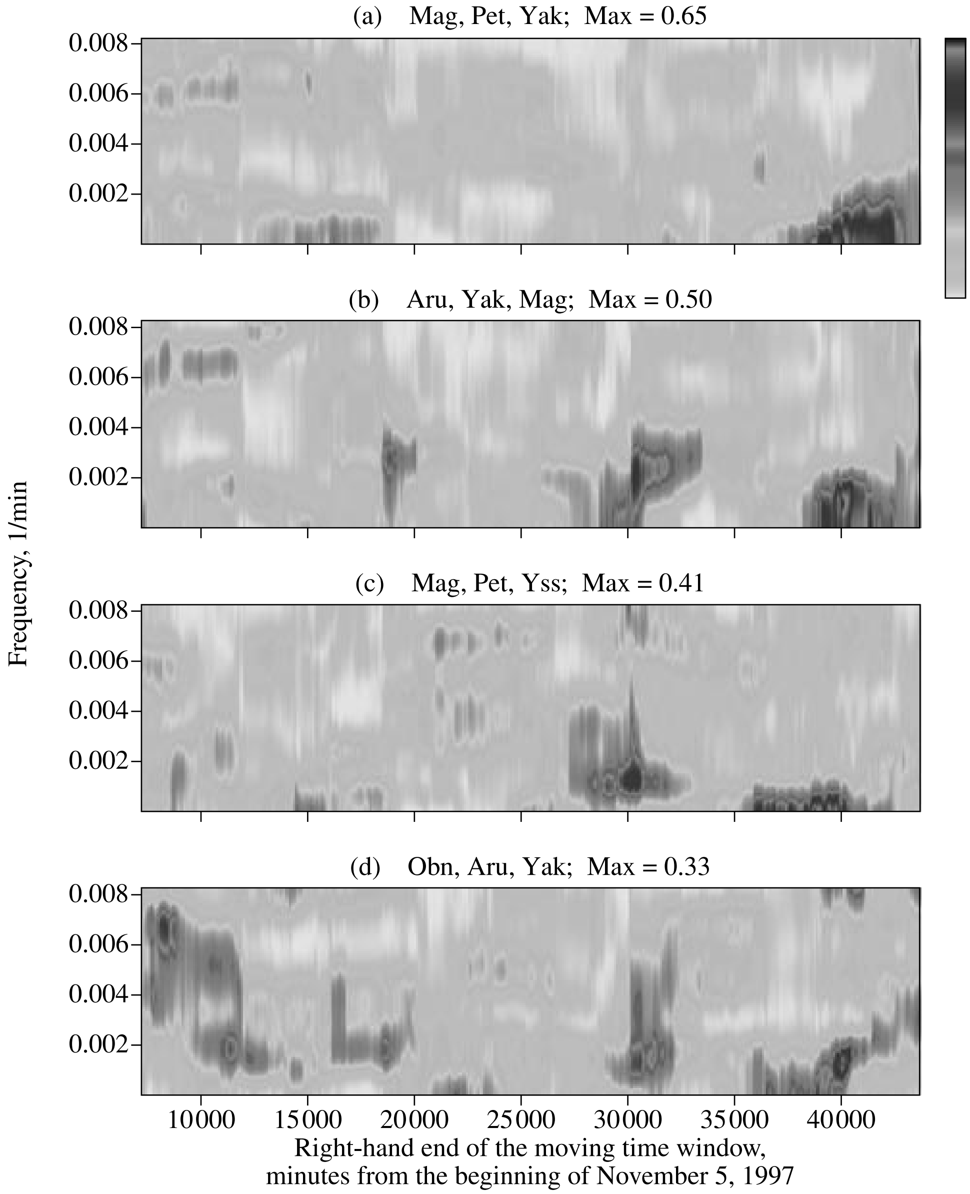

Fig. 6. Frequency–time diagrams of the evolution of the spectral measure of coherence of α* variation spectral series with the estimation in the moving time window 109 samples (5 days) long for various combinations of three simultaneously analyzed stations. Maximum values of the coherence measure are shown in each diagram after the codes of the stations analyzed.

end of the observation interval immediately adjacent to the arrival from the Kronotskii earthquake. Detailed investigations using wavelet expansions [Sobolev et al., 2005] showed that the ends of records obtained at the Obn, Yak, Pet, Yss, and Mag stations contain common pulses in the low frequency range (periods of 10–60 min) that are not associated with arrivals from near or far events.

Figure 5 images the development of a coherence spot on the time–frequency plane before the Kronotskii earthquake obtained by processing a successively increasing number of stations, starting with Pet, Yak, and Mag, closest to the source (Fig. 5a), and ending with all six stations (Fig. 5d). The main coherence pulsation (Fig. 5a) concentrates in the interval 40 000–42 000 min and lies in the lowest frequency part of the spectrum (at periods of 500 to 6000 min). Since the time marks in the diagrams correspond to the right-hand end of the time window 7200 min (5 days) wide, this pulsation corresponds to the time interval 32 800–42 000 in Figs. 1 and 2, or November 28–December 3, 1997. It is noteworthy that, as the moving time window approaches the earthquake occurrence time, the coherence level of α* variations drops, although remaining above statistical background fluctuations. The remaining diagrams in Fig. 5 show that the time length of the low frequency coherence spot increases with an increasing number of stations. Note that in Fig. 5d, additionally including the Aru processing data, the longest coherence pulsation is interrupted in the interval 33 000–34 000 min, which is accounted for by the presence of the low frequency calibrating pulse covering the interval 32 000–32 960 min of the Aru record, as is mentioned above.

The series of diagrams shown in Fig. 6 was calculated to check for the stability of the low frequency coherence pulsation in the vicinity of the time mark 40 000 min by estimating results of various combinations of three stations. Note that, in Fig. 6, it is admissible to compare maximum values of the coherence measure because the number of simultaneously analyzed time series is the same. The highest peak of coherence (0.65) is observed for the Mag, Pet, and Yak stations, at Kronotskii earthquake epicentral distances of 900, 350, and 2050 km, respectively; the peak is lowest (0.32) for the Obn, Aru, and Yak stations, which are farthest from the earthquake source (6800, 5900, and 2050 km, respectively). In all variants shown in Fig. 6, the coherence measure experiences a pulsation in the neighborhood of the time mark 40 000 corresponding to the observation interval November 29–December 3, 1997, i.e., three to seven days before the shock.

An intense series of foreshock activation started on December 3, 1997, preceding the Kronotskii earthquake. As noted in [Sobolev et al., 2005], an increase in the number of regular asymmetric pulses of the minute range of periods was observed in Pet records five days before this earthquake; the same authors report that no anomalous meteorological effects were recorded before the Kronotskii earthquake.

The correlation between records of low frequency microseisms at stations separated by thousands of kilometers (by tens of degrees in longitude) suggests a common source of a regional scale. Since the correlation is best for stations located in the northeastern part of the Far East and Siberia, the source was supposedly located in this region. The problem of its origin remains open.

CONCLUSIONS

Using the evolutionary analysis of the coherence measure of variations in the generalized Hurst exponent realizing the maximums of multifractal singularity spectra of the microseismic noise field, it is shown that the synchronization effect of microseismic noises in northern Eurasia took place three to seven days before the strong Kronotskii (Kamchatka) earthquake of December 5, 1997.

ACKNOWLEDGMENTS

This work was performed within the framework of the program “The Electronic Earth” of the Presidium of the Russian Academy of Sciences and supported by the Russian Foundation for Basic Research (project no. 06-05-64625).

REFERENCES

1. E. Bacry, J. F. Muzy, and A. Arnéodo, “Singularity Spectrum of Fractal Signals: Exact Results,” J. Stat. Phys. **70** (3/4), 635–674 (1993).
2. D. R. Brillinger, *Time Series. Data Analysis and Theory* (Holt, Rinehart and Winston, New York, 1975; Mir, Moscow, 1980) [in Russian].
3. G. Currenti, C. del Negro, V. Lapenna, and L. Telesca, “Multifractality in Local Geomagnetic Field at Etna Volcano, Sicily (Southern Italy),” Natural Hazards and Earth System Sciences **5**, 555–559 (2005).
4. J. Feder, *Fractals* (Plenum Press, New York, 1988; Mir, Moscow, 1991).
5. E. J. Hannan, *Multiple Time Series* (Wiley, New York, 1970; Mir, Moscow, 1974).
6. P. J. Huber *Robust Statistics* (Wiley, New York, 1981; Mir, Moscow, 1984).
7. H. E. Hurst, “Long-Term Storage Capacity of Reservoirs,” Trans. Am. Soc. Civ. Eng. **116**, 770–808 (1951).
8. G. Jenkins and D. G. Watts, *Spectrum Analysis and Its Applications* (Holden Day, San Francisco, 1968; Mir, Moscow, 1972).
9. J. W. Kantelhardt, S. A. Zschiegner, E. Konscienly-Bunde, et al., “Multifractal Detrended Fluctuation Analysis of Nonstationary Time Series,” Physica A **316**, 87–114 (2002).
10. J. W. Kantelhardt, D. Rybski, S. A. Zschiegner, et al., “Multifractality of River Runoff and Precipitation: Comparison of Fluctuation Analysis and Wavelet Methods,” Physica A **330**, 240–245 (2003).
11. A. A. Lyubushin, “Analysis of Canonical Coherences in the Problems of Geophysical Monitoring,” Fiz. Zemli, No. 1, 59–66 (1998) [Izvestiya, Phys. Solid Earth **34**, 52–58 (1998)].
12. A. A. Lyubushin, V. F. Pisarenko, V. V. Ruzhich, and V. Yu. Buddo, “Identification of Periodicities in the Seismic Regime,” Vulkanol. Seismol., No. 1, 62–76 (1998).
13. A. A. Lyubushin, V. F. Pisarenko, M. V. Bolgov, and T. A. Rukavishnikova, “General Effects of Variations in River Runoffs,” Meteorol. Gidrol., No. 7, 76–88 (2003).
14. A. A. Lyubushin, V. F. Pisarenko, M. Bolgov, et al., “Synchronous Variations in the Caspian Sea Level from Shore-Based Data of 1977–1991,” Izv. Ross. Akad. Nauk, Fiz. Atmosf. Okeana **40** (6), 821–831 (2004).
15. S. Mallat, “A Wavelet Tour of Signal Processing” (Academic, San Diego, 1998; Mir, Moscow, 2005).
16. B. B. Mandelbrot, *The Fractal Geometry of Nature* (Freeman, 1983).
17. B. B. Mandelbrot and J. R. Wallis, “Some Long-Term Properties of Geophysical Records,” Water Resources Res. **5**, 321–340 (1969).
18. S. L. Marple, Jr., *Digital Spectral Analysis with Applications* (Prentice-Hall, Englewood Cliffs, New Jersey, 1987; Mir, Moscow, 1990).
19. J. F. Muzy, E. Bacry, and A. Arnéodo, “The Multifractal Formalism Revisited with Wavelets,” Int. J. Bifurc. Chaos **4**, 245–302 (1994).
20. A. Ramírez-Rojas, A. Münoz-Diosdado, C. G. Pavía-Miller, and F. Angulo-Brown, “Spectral and Multifractal Study of Electroseismic Time Series Associated to the M_w = 6.5 Earthquake of 24 October 1993 in Mexico,”

Natural Hazards and Earth System Sci. **4**, 703–709 (2004).

21. V. B. Smirnov, A. V. Ponomarev, Qian Jiadong, and A. S. Cherepanov, "Rhythms and Deterministic Chaos in Geophysical Time Series," Fiz. Zemli, No. 6, 6–28 (2005) [Izvestiya, Phys. Solid Earth **41**, 428–448 (2005)].
22. G. A. Sobolev, "Microseismic Variations Prior to a Strong Earthquake," Fiz. Zemli, No. 6, 3–13 (2004) [Izvestiya, Phys. Solid Earth **40**, 455–464 (2004)].
23. G. A. Sobolev, A. A. Lyubushin, and N. A. Zakrzhevskaya, "Synchronization of Microseismic Variations within a Minute Range of Periods," Fiz. Zemli, No. 8, 3–27 (2005) [Izvestiya, Phys. Solid Earth **41**, 599–621 (2005)].
24. L. Telesca, G. Colangelo, and V. Lapenna, "Multifractal Variability in Geoelectrical Signals and Correlations with Seismicity: A Study Case in Southern Italy," Natural Hazards and Earth System Sci. **5**, 673–677 (2005).
25. D. L. Turcotte, *Fractals and Chaos in Geology and Geophysics* (Univ. Press, New York, 1997), 2nd ed.